Advanced Carbon Journal, 2024, Vol. 1, Iss. 1, 20-32

DOI: 10.62184/acj.jacj1000202420

Review Article

SCIENCE PARK PUBLISHER

Advanced Carbon Journal

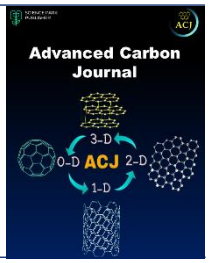

Role of reduced graphene oxide in boosting visible-light-driven photocatalytic activity of $BiVO_4$ nanostructures

Moemen Adel[1,*], Tarek M. Abdel-Fattah[2], Alaa El Din Mahmoud[3,4] and Hesham Hamad[5,6,*]

[1] Department of Chemistry, Faculty of Science, Alexandria University, P.O. Box 426, Ibrahimia, Alexandria 21321, Egypt

[2] Department of Molecular Biology and Chemistry, Christopher Newport University, Newport News, Virginia, 23606, United States of America

[3] Environmental Sciences Department, Faculty of Science, Alexandria University, Alexandria, 21511, Egypt

[4] Green Technology Group, Faculty of Science, Alexandria University, Alexandria, 21511, Egypt

[5] Fabrication Technology Research Department, Advanced Technology and New Materials Research Institute (ATNMRI), City of Scientific Research and Technological Applications (SRTA-City), New Borg El-Arab City, 21934, Alexandria, Egypt

[6] UGR-Carbon, Materiales Polifuncionales Basados en Carbono, Departamento de Quimica Inorganica, Facultad de Ciencias - Unidad de Excelencia Quimica Aplicada a Biomedicina y Medioambiente" Universidad de Granada (UEQ-UGR), 18071 Granada, Spain

Received: 24, 02, 2024; Accepted: 27, 05, 2024; Published: 12, 07, 2024

Abstract

Although monoclinic scheelite bismuth vanadate (m-$BiVO_4$) is a promising photocatalyst due to its low band gap (E_g = 2.4-2.6 eV), significant visible light absorption, and its valence band potential is positive enough for water splitting and pollutants degradation, it has some drawbacks hindering its sole usage in photocatalysis. These drawbacks include low surface conductivity, fast electron/hole (e^-/h^+) pair recombination, low surface area, and low solubility in the aqueous medium. Therefore, m-$BiVO_4$ is composited with reduced graphene oxide (r-GO) to mitigate these drawbacks. r-GO has an extremely large surface area, a high electrical conductivity and can accept and trap electrons from m-$BiVO_4$ via its delocalized conjugated π-system. Such traps lengthen the electron/hole (e^-/h^+) pair lifetime on m-$BiVO_4$ increasing the photocatalytic reactions efficiency on its surface. In addition, the presence of oxygen-containing groups on r-GO helps anchor m-$BiVO_4$ particles on the r-GO layer so the m-$BiVO_4$ particles are more dispersed and display a larger surface area. These oxygenated groups ease the solubilization of anchored m-$BiVO_4$ particles in water by forming hydrogen bonds. In this mini-review, m-$BiVO_4$–r-GO composite applications in photocatalytic water splitting, pollutants degradation, and other reactions will be briefly discussed. Generally, these composites showed remarkable results in reactions that rely on the valence band holes of m-$BiVO_4$, whereas the reactions that depend on conduction band electrons required morphology and size modification for the m-$BiVO_4$ before its compositing with r-GO.

Keywords: Reduced graphene oxide, $BiVO_4$, Photocatalytic degradation, Photocatalytic water splitting, Photocatalytic CO_2 reduction, and Photocatalytic N_2 fixation

Introduction

Bismuth Vanidate ($BiVO_4$) is an attractive photocatalyst because of its narrow band gap, high crystallinity, easy fabrication, photo and chemical stability, and low toxicity [1]. $BiVO_4$ has a highly positive valence band (VB) potential (+2.45 to -2.60 eV) and conduction band (CB) potential value that

DOI: 10.62184/acj.jacj1000202420

ranges from + 0.11 to - 0.05 eV. Both potentials are useful for photo-driven oxygen evolution, water splitting reactions, N_2 fixation, and degradation of organic pollutants [1-4]. The monoclinic scheelite (m-$BiVO_4$) form has the lowest band gap (E_g) (2.4 eV) followed by tetragonal scheelite (2.6 eV) and tetragonal zircon (2.9 eV) structures [5]. Such low E_g values allow a broader visible light absorption and more probable photo-electrons formation. The low E_g is due to the coupling of Bi $6s^2$, $6p^0$ orbitals with the O_{2p} orbitals of VO_4^{3-} and 3d orbitals of V^{5+} causing destabilizing and stabilizing of the valence band maximum (VBM) and the conduction band maximum (CBM), respectively [6]. $BiVO_4$, however, suffers from some drawbacks such as (i) low surface conductivity that causes the rapid recombination of photoproduced e^-/h^+ pair [7], (ii) a small surface area and pore volumes, making extensive photons absorption difficult due to low active sites density added to the reduced substrates adsorption, and (iii) $BiVO_4$ undergoes agglomeration during photocatalysis which impedes its recyclability and further reduces its surface area [8, 9]. The $BiVO_4$ recovery presents another obstacle because it could be degraded and become secondary contaminants in water [10]. Hence, to overcome these drawbacks, m-$BiVO_4$ is doped with metals and non-metals, morphologically controlled, and coupled to another semiconductor forming heterojunctions to reduce the e^-/h^+ recombination. The small surface area and agglomeration are counteracted by supporting m-$BiVO_4$ on a certain support- forming a composite- to disperse it into smaller particles; and so surface area increases, and agglomeration is minimized. [11, 12] In this mini-review, we highlight the influences of compositing r-GO with m-$BiVO_4$ on improving the m-$BiVO_4$ photocatalytic activity in different applications. We started by showing the properties of graphene and why r-GO is preferably composited with m-$BiVO_4$. Then, the mechanism by which r-GO enhances m-$BiVO_4$ photocatalytic properties is shown. The applications of m-$BiVO_4$/r-GO composite are ordered according to their frequent appearance in literature. Photocatalytic degradation of pollutants by this composite is first discussed followed by other applications including photocatalytic water splitting, nitrate formation, and CO_2 reduction and photoesterification.

$BiVO_4$ - carbon support composite

Carbon supports are classified dimensionally into zero dimensional (0D) (such as fullerenes), one dimensional (1D) (such as carbon nanotubes (CNT)), two dimensional (2D) (such as graphene family), and three dimensional (3D) structures (such as graphite) [13-15]. Carbon supports are merited by their boosted adsorption performance. They can reduce a semiconductor band gap and promote e^-/h^+ charge separation by the as-formed carbon-based Schottky-junction between the semiconductor and highly conductive nanocarbon supports [16]. More precisely, combining different carbon-rich materials with semiconductors produces interesting synergistic effects in addition to compensating for the drawbacks of the individual semiconductor materials. These effects include band gap narrowing, co-catalysis, increased adsorption and active sites, electron accepting and transporting channels [17]. 0D structures have a large surface area whereas 1D structures have a high aspect ratio and high electric conductivity [18, 19]. A 2D carbon nanosheet, such as graphene (a sp^2-hybridized carbon) has significantly higher optical transmittance, conductivity (~5000 $W\ m^{-1}\ K^{-1}$), electron mobility (200,000 $cm^2\ V^{-1}\ s^{-1}$), theoretical specific surface area (~2600 $m^2\ g^{-1}$), and a more appropriate work function (4.42 eV) for H_2 evolution than the 0D and 1D carbonaceous materials [20]. 2D combines the properties of 0D and 1D, adding to its greater interfacial contact. Although graphene has an extremely high surface area and electric and thermal conductivity due to its zero-band gap and extended sp^2 carbon hybridization, it can restack forming graphene aggregates that reduce the graphene surface area needed to support and disperse $BiVO_4$. So, controlled graphene oxidation is aimed to acquire graphene oxygenated functional groups to bond to $BiVO_4$ and disperse graphene in aqueous systems. Oxidation should be controlled otherwise the extreme oxidation can convert graphene to graphene oxide (GO) which is electrically insulating. Graphene is firstly oxidized to GO that is then

partially reduced to give reduced graphene oxide (r-GO). r-GO has graphene advantages and good water dispersibility [21].

$BiVO_4$-rGO

The combination of $BiVO_4$ and rGO has been widely shown to be a promising strategy for favoring the charge transfer and inhibiting the charge recombination process, thereby leading to boosted photocatalytic activity [22, 23]. Reduced graphene oxide (rGO) has been investigated more because it combines great adsorptive powers with the inherited properties of graphene [24]. GO contains even higher adsorption and electron-accepting abilities due to having more oxygen-containing functional groups, but it is an insulator [24, 25]. In other words, the rGO increases the $BiVO_4$ surface area and elongates the lifetime of separated e^-/h^+ pairs via accepting electrons from $BiVO_4$ (trapper and a co-catalyst) and so widens the $BiVO_4$ photo-absorption range and enhances the accepted electrons mobility. Electron mobility occurs via the rGO extended π-π conjugation system. Careful consideration should be taken when compositing rGO with $BiVO_4$ as too many rGO layers can adhere to the $BiVO_4$ and block the visible light pathway to the $BiVO_4$. rGO layers, in addition, can stack due to hydrogen bond formation between oxygen-containing groups, Vander Waal, and π-π stacking interactions. This stacking reduces the rGO surface area and causes $BiVO_4$ agglomeration [26-29]. Improved visible-light photocatalytic activity results from $BiVO_4$ effective narrow band gap, the trapping of electrons by r-GO and the wide r-GO surface area that allows extensive pollutants adsorption via *π-π* and hydrogen bonds interactions.

Various applications of $BiVO_4$ coupled with rGO composite photocatalysts have occurred like photocatalytic degradation of pollutants, water splitting, N_2 fixation, and CO_2 reduction. Some of these applications rely on $BiVO_4$ holes as in photocatalytic pollutants degradation and photocatalytic water splitting, others rely on $BiVO_4$ electrons as in photocatalytic CO_2 reduction, and others depend on both holes and electrons as photo esterification.

Photocatalytic degradation of pollutants

Photocatalytic degradation of organic pollutants using photocatalysts has been widely used for air and water purification [30, 31]. Table 1 summarizes the photocatalytic activities of $BiVO_4$ with rGO-based photocatalysts for degradation of organic pollutants on various conditions including band gap, dose of catalyst, rate constants, reactive oxygen species, type and power of light source, and cycling numbers. In photocatalytic degradation, rGO elongates the photo-induced e^-/h^+ pairs of m-$BiVO_4$ via accepting electrons from the m-$BiVO_4$ CB and thus holes accumulate in the VB [32, 33]. The transferred electrons are injected into adsorbed O_2 molecules on rGO forming superoxide anion (O_2^{-}) which reacts with water molecules forming hydroxide radical (•OH). rGO absorbs O_2 due to the existence of surface oxygen containing groups. The accumulated holes react directly with the substrate or with water forming •OH. The O_2^{-} is formed only on rGO as the $BiVO_4$ CB is less negative than that of O_2/ O_2^{-} reaction (-0.33 V vs NHE), whereas rGO mobiles accepted electrons easing their transfer to absorbed O_2. •OH is formed from the holes when they have more positive potential than that needed for water oxidation (H_2O/•OH of 2.70 V vs NHE), otherwise holes directly attack the substrate. Also, ˙OH can be formed from reacting hydroxide anion (OH^-**)** with holes (OH^-/•OH of 1.99 V vs NHE). The substrate here is referred to the organic pollutants as antibiotics, phenols and microorganisms [11, 12, 22, 23]. That is why in Table 1 the same pollutant, such as Methylene Blue (MB), may undergo degradation by h^+, O_2^{-} and •OH and in other cases by holes and O_2^{-} only. In Table 1, all the E_g values of the composite are lower than that of the $BiVO_4$ only due to: i) formation of Bi-C covalent bonds between the $BiVO_4$ and rGO and increased $BiVO_4$ crystallinity; ii) formation of an internal electric field between the m-$BiVO_4$ and the rGO where the rGO fermi-level equilibrates with that of m-$BiVO_4$ causing the bending of m-$BiVO_4$ CB and VB downwards. These factors ease the electron migration from m-$BiVO_4$ to rGO so that the e^-/h^+ pair lifetime is elongated allowing more time for the degradation of pollutants that need multi-electrons to change to benign products [34]; and (iii) increasing the surface area of exposed m-

Advanced Carbon Journal, 2024, Vol. 1, Iss. 1, 20-32

DOI: 10.62184/acj.jacj1000202420

$BiVO_4$ to different substrates [11, 12, 23]. For example, Duan et al. (2022) studied the impact of compositing r-GO with m-$BiVO_4$ on the photocatalytic degradation of rhodamine B (RhB). The study stated that the composite achieved 98.3% degradation efficiency, in 180 min., which was 1.3 times higher than that of m-$BiVO_4$. The E_g reduced from 2.6 to 2.21 eV for the m-$BiVO_4$ and the composite, respectively. On the other hand, the composite specific surface area was more than double that of sole m-$BiVO_4$ which increases the RhB adsorption [22]. The general mechanism of photocatalytic degradation of organic pollutants and photo reduction of metal ions such as Cr(VI) as a model pollutant by $BiVO_4$ - r-GO is presented in Figure 1.

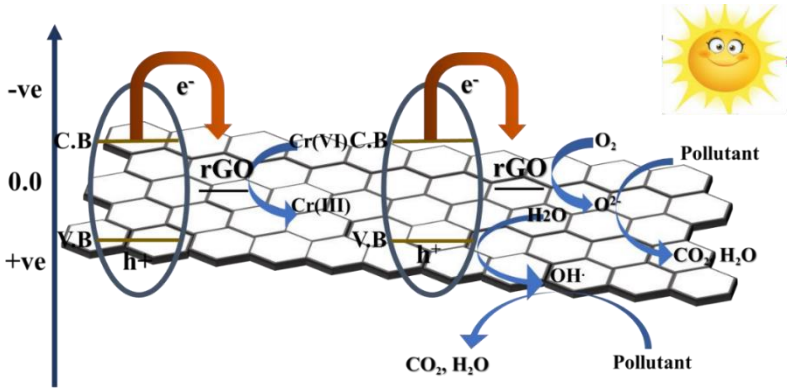

Figure 1. Charge separation mechanisms in the $BiVO_4$-rGO system for photodegradation of organic pollutants and photoreduction of Cr (VI) ions.

Abo El-Yazeed et al. (2021) showed that if m-$BiVO_4$ is calcined to 700 °C, its E_g value reduces from 2.45 eV to 1.88 eV. Furthermore, when this calcined m-$BiVO_4$ binds to rGO, the E_g is lowered to 1.59 eV which is the lowest E_g value reported. Consequently, such composite shows extremely high photoabsorption, and more accumulated e^-/h^+ pairs. In addition, the times needed for 100% and 79% degradation of methylene blue (MB) and RhB by this catalyst were the shortest reported durations with 30 and 50 minutes for MB and RhB, respectively [34].

Azad et al. (2019) studied the photocatalytic reduction of some nitrobenzenes and nitrophenols to the corresponding amines using m-$BiVO_4$ - r-GO composite. The composite attained 100% conversion efficiency compared to only 11% by m-$BiVO_4$. The E_g was lowered from 2.41 to 2.08eV for the m-$BiVO_4$ and the composite, respectively. Also, the rate of conversion increased by 10 times that of m-$BiVO_4$ [35].

Kumar et al. (2021) studied the piezoelectric behavior of m-$BiVO_4$ and its impact on elongatingthe lifetime of e^-/h^+ pair added to rGO impact on MB photodegradation. They concluded that high adsorption capabilities and the long e^-/h^+ pair lifetime on m-$BiVO_4$ surface boosted the rate of MB degradation at low light intensities. Piezocatalysis involves applying mechanical impact on an anisotropic (have anionic and cation crystal mismatch) semiconductor that polarizes the semiconductor into positively and negatively charged dipoles. Such polarization aids in separatingthe photoinduced e^-/h^+ pair of m-$BiVO_4$ that elongates its lifetime. By the way, m-$BiVO_4$ has crystal mismatches and so anisotropy exists. Mechanical stress can be induced by sonication. Sonication produces bubbles of extremely high energy that burst onto m-$BiVO_4$ generating mechanical stresses. The collapsing of these bubbles generates very high temperatures (4000- 5000K) that are enough to thermally excite m-$BiVO_4$ electrons (sonocatalysis) and produce photons that excite the same electrons (sonophotocatalysis). These latter influences cause more e^-/h^+

DOI: 10.62184/acj.jacj1000202420

pairs to form [36, 37]. The general mechanism of photocatalytic degradation of organic pollutants and photo reduction of metal ions by $BiVO_4$ - r-GO is presented in Figure 2.

Table 1. $BiVO_4$-rGO composite for photodegradation of organic pollutants

Target Pollutant	Reactive Oxygen Species (ROS)	Light Source	Eg (eV)	Time (min.)	K_{app}	Catalyst Dose (g/L)	Cycles	Degradation (%)	Ref.
RhB and MO	---	1 sun illumination (100 mW/cm^2)	---	120		---	5	---	[38]
MB	O_2^- and •OH	300 W xenon lamp	2.45	190		---	3	96.9	[39]
RhB	•OH, O_2^-		2.1	180		---	4	98.3	[22]
Acetaminophen	•OH, h^+		2.45	150	0.0141 min^{-1}	---	4		[27]
MB and RhB	•OH, h^+, O_2^-		1.59	30 (MB), 50 (RhB)	(MB) 0.09804 min^{-1}, (RhB) 0.05304 min^{-1}	1	5	100 (MB), 79 (RhB).	[34]
BPA	•OH	(16.7 mW.cm $^{-2}$)	2.44		4.5 × 10^{-2} mmol. g^{-1}. min $^{-1}$	0.4		72	[23]
RhB	•OH, O_2^-	Direct sunlight.	2.1	120	2.1606 x 10^{-2} min^{-1}	0.4		92.51	[11]
Caffeine		UV-C led lamp.	2.02	240	7 × 10^{-3} s^{-1}	---		100	[28]
Tetracycline	h^+,O_2^-	55 W fluorescent lamp.	2.21	50		---		17	[12]
Reactive Black 5	h^+,O_2^-	1 kW xenon lamp	2.05	3600		---		95	[32]
MB	•OH, O_2^-	xenon lamp of 300 W	2.27	210	0.0046 min^{-1}	1	3	94	[29]
2,4-dichlorophenol	•OH, h^+	simulated solar irradiation	---		0.00184 min^{-1}	1		55	[40]
Antifouling, MB	•OH, O_2^-		2.11	240	0.047	---		94.77 (MB)	[2]
MB	O_2^-	150 W	2.40	180	0.0088	---		82	[36]
MB	O_2^-	---	---	180	---	---		~81	[37]
MB	O_2^-	150 W	---	180	---	---		~52	[41]
MB		1-kW Xe-lamp	---	90	---	---		97	[42]
Hexavalent chromium reduction		500 W Xe lamp	2.23		0.1560	---		97.6	[26]

Advanced Carbon Journal, 2024, Vol. 1, Iss. 1, 20-32

DOI: 10.62184/acj.jacj1000202420

Review Article

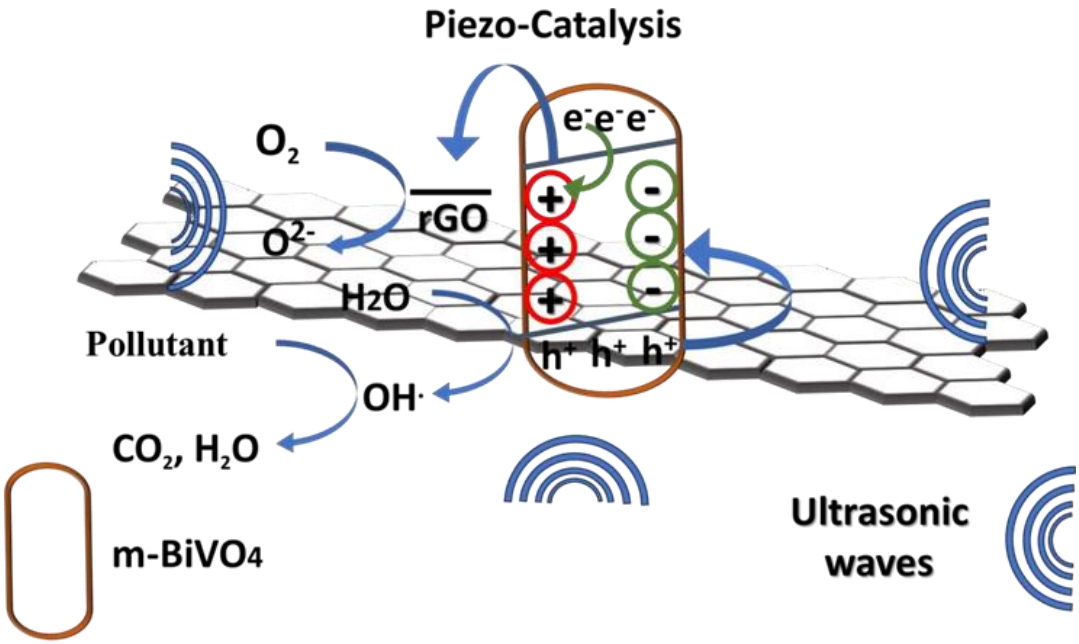

Figure 2. Piezo-catalytic reaction mechanism using the m-$BiVO_4$-rGO system.

Photocatalytic water splitting and nitrate formation

Most of the photoelectrochemical reactions are undertaken in a photoelectrochemical cell where the photoanode carries the m-$BiVO_4$-rGO composite, and a positive applied potential bias attracts photoinduced electrons, causing holes accumulation that then react with water or N_2 leading to O_2 evolution or nitrates formation, respectively. On the other hand, photoinduced electrons migrate to the cathode where hydrogen evolution takes place in the presence of H^+ or H_2O [43, 44]. Table 2 summarizes the photocatalytic activities of m-$BiVO_4$-rGO photocatalysts for H_2 production and nitrate formation on various conditions. Yaw et al. (2020) achieved a very high photocurrent (2.1 mA/cm^2) of hydrogen evolved using m-$BiVO_4$-rGO- via sandwiching rGO between m-$BiVO_4$ (n- type) and vanadium pentoxide (V_2O_5) (p-type). m-$BiVO_4$ is the electron sensitizer that transfers electrons to V_2O_5 via rGO and in reverse, the V_2O_5 transfers holes to the m-$BiVO_4$. These two transfers elongate the electron-hole pairs lifetime formed on m-$BiVO_4$ and accumulate more holes on m-$BiVO_4$ and more electrons on V_2O_5, thereby easing higher O_2 and H_2 production rates, respectively. Figure 3 represents the mechanism of charge separation for photocatalytic water splitting in the system of m-$BiVO_4$-rGO composite [44]. Liu et al. (2022) studied the impact of engineering oxygen vacancies (O_v) defects on the m-$BiVO_4$ surface on H_2O photooxidation where O_v trap photo-induced electrons elongating e^-/h^+ pair lifetime, added to the impact of contacting rGO to m-$BiVO_4$. They stated that the photo-absorption intensifies on this composite due to generating a defect state below the CBM easing an intra-band transition at lower E_g values. They also added that the O_v present in coordination-unsaturated metal atom sites adsorb H_2O molecules easily increasing the rate of $_{O2}$ evolution. The percentage of O_2 evolved was interestingly 209% higher than that of normal m-$BiVO_4$. Also, the apparent quantum yield was ~23.19% [43]. Shao et al. (2022) [45] studied using 2D m-$BiVO_4$ - 2D rGO composite relying on the marvelous advantages of having a 2D interfacial contact with an extensive surface area on N_2 photooxidation to NO_3^-. The apparent quantum efficiency was 0.64 and the rate of N_2 oxidation was ~8 times higher on the composite than the normal m-$BiVO_4$.

Advanced Carbon Journal, 2024, Vol. 1, Iss. 1, 20-32

DOI: 10.62184/acj.jacj1000202420

Review Article

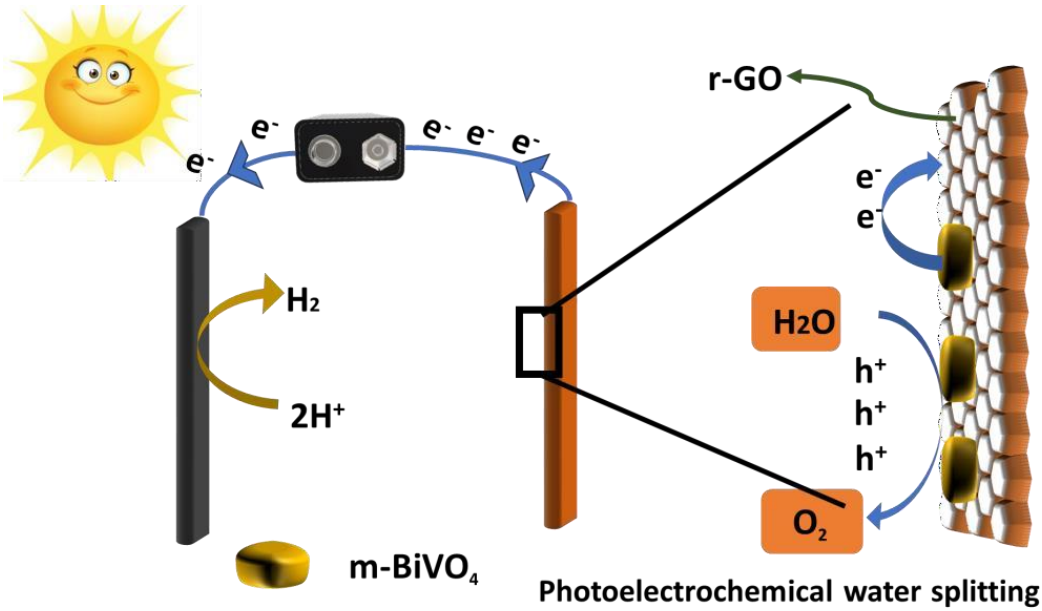

Figure 3. Charge separation mechanism for photocatalytic water splitting in the m-$BiVO_4$-rGO.

Photocatalytic CO_2 reduction

From the perspective of developing sustainable energy, one of the best ways to address the serious problems of global warming and fossil fuel shortages would be to use solar energy to convert the rapidly rising greenhouse gases into valuable energy-bearing compounds (such as carbon monoxide (CO), methane, and methanol). CO_2 photoreduction to C_1 products on m-$BiVO_4$ is unfeasible as its CB-minimum potential is less negative than CO_2 reduction potential [46,47]. So, the CB of m-$BiVO_4$ should be negatively uplifted to overcome the CO_2 potential. Such uplift is attained by further distorting the m-$BiVO_4$ to destabilize both the CB-minimum and the VB-maximum. Doing so, CB is negatively raised while E_g is kept as narrow as possible.

Again, rGO accepts electrons from the m-$BiVO_4$ elongating the e^-/h^+ pairs lifetime to allow the multi-electrons CO_2 reduction to occur on m-$BiVO_4$. For example, Chen et al., 2019 [48] studied using m-$BiVO_4$ quantum dots (BQDs) to elevate the CB-minimum to negative potentials that surpass the CO_2 reduction potential. Quantum dots are merited by the property of enlarging the E_g values as their sizes are reduced. In this work, the E_g increases from 2.4 eV for bulk m-$BiVO_4$ to 2.7 eV for BQDs. BQDs also dramatically increase the surface area of m-$BiVO_4$ allowing more CO_2 adsorption. Again, the rGO accepts electrons from BQDs, thereby elongating the lifetime of e^-/h^+ pairs.

DOI: 10.62184/acj.jacj1000202420

Table 2. $BiVO_4$-rGO composites for water splitting, CO_2 reduction and N_2 fixation reactions

Application	Type of Photocatalyst (powder or thin film)	Light Source (Power)	Stability	E_g (eV)	Photocurrent	Reaction time	Ref.
H_2 production	Powder	simulated solar light	29 on–off irradiation cycles	2.48 (BVO/rGO-5%), 2.44 for BVO/rGO-10%.	377.9 µA cm^{-2}, (BVO/rGO-5%), BVO/rGO-10% (554.4 µA cm^{-2})		[33]
H_2 production	Thin film	150 W with an output intensity of 100 mW/cm^2.			2.1 mA/cm^2		[44]
H_2 production	Powder	1-kW Xe-lamp				2 hours	[43]
Photo-Esterification	Powder	1040 W/m^2	6 cycles			3 hours	[49]
CO_2 reduction	Powder	300 W	5 cycles	2.7			[48]
N_2 fixation to nitrates	Powder	---	12 hours long term stability		1.45 mg h^{-1} g^{-1}		[45]
H_2O_2 production	Powder	---	4 cycles and each cycle is 3 hours.	2.06	1.55 µA/cm^2		[4]
Water Oxidation	Powder	---		O_v-poor BG= 2.49, O_v-rich BG= 2.51	The O_v-rich BG exhibited 650.0 µmol/g of O_2 yield	5 hours	[43]
H_2 production		200 W Hg-Xe arclamp		2.44	11.5 µmol. g^{-1}. h^{-1}		[23]

Conclusion and future prospective

In summary, this mini-review highlights the versatile properties and potential applications of m- $BiVO_4$-rGO composite photocatalysts. Obviously, m-$BiVO_4$ solely attains various reactions at low rates due to its low surface conductivity, adsorption ability and high rates of e^-/h^+ pairs recombination. $BiVO_4$ composites have proven to be one of the most promising photocatalyst candidates for various applications. There is no doubt that the rapid growth of $BiVO_4$ based composite photocatalysts will occur in the near future. To date, although considerable progress has been achieved in the recent years, there are still many challenges to deeply understand the enhancement of the graphene family when coupled with $BiVO_4$. Graphene supports, especially rGO, are used to mitigate such drawbacks as they have oxygen functional groups that can disperse m- $BiVO_4$ and achieve intimate contact that eases electrons transfer from the m-$BiVO_4$ CB to graphene Fermi level. Notably, most of the m-$BiVO_4$ is composited with rGO and such composite is used mostly in photocatalytic reactions where oxidation is targeted such as photocatalytic degradation and water splitting. This is because the VBM potential of m-$BiVO_4$ is sufficiently positive to overcome the potential barriers needed for these reactions. In such reactions, rGO accepts electrons that transfer to adsorbed O_2 forming superoxides that react with the substrate

and/or these superoxides are converted to hydroxyl radicals that also attack the target substrate. However, the cyclability tests are not significantly done for these composites, and their stability needs to be further analyzed.

List of Abbreviations

VBM	Valence Band Maximum
CBM	Conduction Band Minimum
MB	Methylene Blue
RhB	Rhodamine B
BPA	Bis Phenol A
TC	Tetracycline
BQDs	Bismuth Quantum Dots
r-GO	Reduced graphene oxide
O_v	Oxygen Vacancy
e^-/h^+	Electron hole pair
BG	Bismuth vanadate-Graphene

Acknowledgments

Hesham Hamad gratefully thanks the financial support from the MAEC-AECID Spanish fellowship. Dr. Tarek M. Abdel-Fattah acknowledges Lawrence J. Sacks Professorship in Chemistry.

Authors Information

Corresponding Author: Moemen Adel*
E-mail: moemen.adel@alexu.edu.eg
Corresponding Author: Hesham Hamad*
E-mails: hhamad@srtacity.sci.eg, heshamaterials@hotmail.com
ORCID iD: 0000-0002-2434-8904

References

[1] Łęcki, T., Hamad, H., Zarębska, K., Wierzyńska, E., and Skompska, M., (2022). Mechanistic insight into photochemical and photoelectrochemical degradation of organic pollutants with the use of $BiVO_4$ and $BiVO_4$/Co-Pi, Electrochim Acta. 434141292. https://doi.org/10.1016/j.electacta.2022.141292.

[2] Esmaili, Z., Sadeghian, Z., and Ashrafizadeh, S.N., (2023). Anti-fouling and self-cleaning ability of $BiVO_4$/rGO and $BiVO_4$/g-C_3N_4 visible light-driven photocatalysts modified ceramic membrane in high performance ultrafiltration of oily wastewater, J. Memb. Sci., 688. https://doi.org/10.1016/j.memsci.2023.122147.

[3] Zhu, P., Zhang, S., Liu, R., Luo, D., Yao, H., Zhu, T., and Bai, X., (2022). Investigation of an enhanced Z- scheme magnetic recyclable $BiVO_4$/GO/$CoFe_2O_4$ photocatalyst with visible-light-driven for highly efficient degradation of antibiotics, J. Solid State Chem., 314 123379. https://doi.org/10.1016/j.jssc.2022.123379.

[4] Dhabarde, N., Carrillo-Ceja, O., Tian, S., Xiong, G., Raja, K., and Subramanian, V.R., (2021). Bismuth vanadate encapsulated with reduced graphene oxide: A nanocomposite for optimized photocatalytic hydrogen peroxide generation, J. Phys. Chem. C., 125. 23669–23679. https://doi.org/10.1021/acs.jpcc.1c05315.

[5] Sajid, M.M., Assaedi, H., and Zhai, H., (2023). Transition metal vanadates (MVO; M=Bi, Fe, Zn) synthesized by a hydrothermal method for efficient photocatalysis, J. Mater. Sci.: Mater. Electron. 34. https://doi.org/10.1007/s10854-023-09923-5.

[6] Dolgos, M.R., Paraskos, A.M., Stoltzfus, M.W., Yarnell, S.C., and Woodward, P.M., (2009). The electronic structures of vanadate salts: Cation substitution as a tool for band gap manipulation, J. Solid State Chem., 182. 1964–1971. https://doi.org/10.1016/j.jssc.2009.04.032.

[7] Abdi, F.F., Savenije, T.J., May, M.M., Dam, B., and Van De Krol, R., (2013). The origin of slow carrier transport in $BiVO_4$ thin film photoanodes: A time-resolved microwave conductivity study, J. Phys. Chem. Lett., 4. 2752–2757. https://doi.org/10.1021/jz4013257.

[8] Ma, C., Seo, W.C., Lee, J., Kim, Y., Jung, H., and Yang, W., (2021). Construction of quantum dots self- decorated $BiVO_4$/reduced graphene hydrogel composite photocatalyst with improved photocatalytic performance for antibiotics degradation, Chemosphere. 275, 130052. https://doi.org/10.1016/j.chemosphere.2021.130052.

[9] Ma, C., Xie, Z., Seo, W.C., Ud Din, S.T., Lee, J., Kim, Y., Jung, H., and Yang, W., (2021). Carbon dot- coupled $BiVO_4$/reduced graphene hydrogel for significant enhancement of photocatalytic activity: Antibiotic degradation and CO_2 reduction, Appl. Surf. Sci., 565, 150564. https://doi.org/10.1016/j.apsusc.2021.150564.

[10] Wang, R., Wu, Z., Chen, X., Cheng, B., and Ou, W., (2023). Water purification using a $BiVO_4$/graphene oxide multifunctional hydrogel based on interfacial adsorption-enrichment and photocatalytic antibacterial activity, Ceram Int., 49, 9657–9671. https://doi.org/10.1016/j.ceramint.2022.11.137.

[11] Kannan, N., Venkatesh, P.S., Babu, M.G., Paulraj, G., and Jeganathan, K., (2023). Hydrothermally synthesized rGO-$BiVO_4$ nanocomposites for photocatalytic degradation of RhB, Chemical Physics Impact. 6, 100230. https://doi.org/10.1016/j.chphi.2023.100230.

[12] Soltani, T., Tayyebi, A., and Lee, B.K., (2019). Photolysis and photocatalysis of tetracycline by sonochemically heterojunctioned $BiVO_4$/reduced graphene oxide under visible-light irradiation, J. Environ. Manag., 232, 713–721. https://doi.org/10.1016/j.jenvman.2018.11.133.

[13] Li, Y.-H., Ding, J., Luan, Z., Di, Z., Zhu, Y., Xu, C., Wu, D., and Wei, B., (2003). Competitive adsorption of Pb^{2+}, Cu^{2+} and Cd^{2+} ions from aqueous solutions by multiwalled carbon nanotubes, Carbon. 41, 2787–2792. https://doi.org/10.1016/S0008-6223(03)00392-0.

[14] Deng, X., Lü, L., Li, H., and Luo, F., (2010). The adsorption properties of Pb(II) and Cd(II) on functionalized graphene prepared by electrolysis method, J. Hazard. Mater. 183, 923– 930. https://doi.org/10.1016/j.jhazmat.2010.07.117.

[15] Benjedim, S., Romero-Cano, L.A., Hamad, H., Bailón-García, E., Slovák, V., Carrasco- Marín, F., and Pérez-Cadenas, A.F. (2021). Synthesis of magnetic adsorbents based carbon highly efficient and stable for use in the removal of Pb(II) and Cd(II) in aqueous solution, Mater. 14. https://doi.org/10.3390/ma14206134.

[16] Ye, Y., and Dai, L., (2021). Graphene-based Schottky junction solar cells, J. Mater. Chem., 22, 24224–24229. https://doi.org/10.1039/C2JM33809B.

[17] Cao, S., and Yu, J., (2016). Carbon-based H_2-production photocatalytic materials, J. Photochem. Photobiol. C: Photochem. Rev., 27, 72–99. https://doi.org/10.1016/j.jphotochemrev.2016.04.002

[18] Xiao, J., Han, J., Zhang, C., Ling, G., Kang, F., and Yang, Q., (2022). Dimensionality, function and performance of carbon materials in energy storage devices, Adv. Energy Mater. 12, 2100775. https://doi.org/10.1002/aenm.202100775.

[19] Xu, Q., Li, W., Ding, L., Yang, W., Xiao, H., and Ong, W.-J., (2019). Function-driven engineering of 1D carbon nanotubes and 0D carbon dots: mechanism, properties and applications, Nanoscale. 11, 1475–1504. https://doi.org/10.1039/C8NR08738E.

[20] Xu, J., He, S., Zhang, H., Huang, J., Lin, H., Wang, X., and Long, J. (2015). Layered metal–organic framework/graphene nanoarchitectures for organic photosynthesis under visible light, J Mater Chem A., 3, 24261–24271. https://doi.org/10.1039/C5TA06838J.

[21] Eigler, S., and Hirsch, A., (2014). Chemistry with graphene and graphene oxide—challenges for synthetic chemists, Angewandte Chemie International Edition 53, pp. 7720–7738. https://doi.org/10.1002/anie.201402780

[22] Duan, A., Hou, X., Yang, M.. Yu, H., Yang, Y., Ma, Q., and Dong, X., (2022). EDTA-2Na assisted facile synthesis of monoclinic bismuth vanadate (m-$BiVO_4$) and m-$BiVO_4$/rGO as a highly efficient visible-light-driven photocatalyst, Mater. Lett., 311, 131498. https://doi.org/10.1016/j.matlet.2021.131498.

[23] Sekar, K., Kassam, A., Bai, Y., Coulson, B., Li, W., Douthwaite, R.E., Sasaki, K., and Lee, A.F., (2021). Hierarchical bismuth vanadate/reduced graphene oxide composite photocatalyst for hydrogen evolution and bisphenol A degradation, Appl. Mater. Today. 22, 100963. https://doi.org/10.1016/j.apmt.2021.100963.

[24] Zhao, J., Liu, L., and Li, F. (2014). Graphene Oxide: Physics and Applications, Springer; 2015th edition. https://doi.org/10.1007/978-3-662-44829-8.

[25] Jiang, D., and Chen, Z., (2013). Graphene chemistry: theoretical perspectives, John Wiley & Sons.

[26] Balakumar, V., Chuaicham, C., Sasaki, K., and Sekar, K., (2021). Fabrication of $BiVO_4$/ reduced graphene oxide photocatalyst for hexavalent chromium reduction under visible region, Mater. Today: Proc., 50, 400–405. https://doi.org/10.1016/j.matpr.2021.11.381.

[27] Sun, J., Wang, C., Shen, T., Song, H., Li, D., Zhao, R., and Wang, X., (2019). Engineering the dimensional interface of $BiVO_4$-2D reduced graphene oxide (RGO) nanocomposite for enhanced visible light photocatalytic performance, J. Nanomater. 9, 907. https://doi.org/10.3390/nano9060907.

[28] Prado, T.M., Silva, F.L., Carrico, A., Lanza, M.R., de V., Fatibello- Filho, O., and Moraes, F.C., (2022). Photoelectrocatalytic degradation of caffeine using bismuth vanadate modified with reduced graphene oxide, Mater Res Bull 145, 111539. https://doi.org/10.1016/j.materresbull.2021.111539.

[29] Sajid, M.M., Shad, N.A., Javed, Y., Khan, S.B., Zhang, Z., and Amin, N., (2020). Study of the interfacial charge transfer in bismuth vanadate/reduce graphene oxide ($BiVO_4$/rGO) composite and evaluation of its photocatalytic activity, Res. Chem. Intermediat. 46, 1201–1215. https://doi.org/10.1007/s11164-019-04029-2.

[30] Hamad, H., Elsenety, M.M., Sadik, W., El-Demerdash, A.-G., Nashed, A., Mostafa, A., and Elyamny, S., (2022). The superior photocatalytic performance and DFT insights of S-scheme CuO@TiO_2 heterojunction composites for simultaneous degradation of organics, Sci Rep 12, 2217. https://doi.org/10.1038/s41598-022-05981-7.

[31] Hamad, H., Bailón-García, E., Pérez-Cadenas, A.F., Maldonado-Hódar, F.J., and Carrasco- Marín, F., (2020). ZrO_2-TiO_2/Carbon core-shell composites as highly efficient solar-driven photo- catalysts: An approach for removal of hazardous water pollutants, J Environ Chem Eng 8, 104350. https://doi.org/10.1016/j.jece.2020.104350.

[32] Qian, J., Cao, L., Hu, X., Li, Y., Wang, R., Shen, M., and Qu, J., (2022). Preparation of RGO film based $BiVO_4$ (040) composites with photocatalytic properties, Z Anorg Allg Chem 648, 1–10. https://doi.org/10.1002/zaac.202200161.

[33] Soltani, T., Tayyebi, A., and Lee, B.-K., (2018). Efficient promotion of charge separation with reduced graphene oxide (rGO) in $BiVO_4$/rGO photoanode for greatly enhanced photoelectrochemical water splitting, Sol. Energy Mater.185, 325–332. https://doi.org/10.1016/j.solmat.2018.05.050.

[34] Abo El-Yazeed, W.S., El-Hakam, S.A., Salah, A.A., and Ibrahim, A.A., (2021). Fabrication and characterization of reduced graphene-$BiVO_4$ nanocomposites for enhancing visible light photocatalytic and antibacterial activity, J

Photochem Photobiol A Chem 417, 113362. https://doi.org/10.1016/j.jphotochem.2021.113362.

[35] Azad, R., Bezaatpour, A., Amiri, M., Eskandari, H., Nouhi, S., Taffa, D.H., Wark, M., Boukherroub, R., and Szunerits, S., (2019). Excellent photocatalytic reduction of nitroarenes to aminoarenes by $BiVO_4$ nanoparticles grafted on reduced graphene oxide (rGO/$BiVO_4$), Appl Organomet Chem 33. https://doi.org/10.1002/aoc.5059.

[36] Porwal, C., Verma, S., Kumar, M., Chauhan, V.S., and Vaish, R., (2023). Bismuth vanadate-reduced graphene oxide-polyvinylidene fluoride electrospun composite membrane for piezo- photocatalysis, Nano-Struct. Nano-Objects. 34, 100969. https://doi.org/10.1016/j.nanoso.2023.100969.

[37] Kumar, M., Singh, G., and Vaish, R., (2021). A reduced graphene oxide/bismuth vanadate composite as an efficient piezocatalyst for degradation of organic dye, Mater Adv 2, 4093–4101. https://doi.org/10.1039/d1ma00284h.

[38] Noureen, L., Xie, Z., Hussain, M., Li, M., Lyu, Q., Wang, K., Zhang, L., and Zhu, J., (2021). $BiVO_4$ and reduced graphene oxide composite hydrogels for solar-driven steam generation and decontamination of polluted water, Sol. Energy Mater. 222, 110952. https://doi.org/10.1016/j.solmat.2020.110952.

[39] Guo, Q., Sun, H., Zhang, L., and Li, D., (2021). Cotton fabric-based rGO/$BiVO_4$ recyclable photocatalytic nanocomposites for dye degradation under visible light, Comp.Comm. 27, 100846. https://doi.org/10.1016/j.coco.2021.100846.

[40] Tu, L., Hou, Y., Yuan, G., Yu, Z., Qin, S., Yan, Y., Zhu, H., Lin, H., Chen, Y., and Wang, S., (2020). Bio-photoelectrochemcial system constructed with $BiVO_4$/RGO photocathode for 2,4- dichlorophenol degradation: $BiVO_4$/RGO optimization, degradation performance and mechanism, J Hazard Mater 389, 121917. https://doi.org/10.1016/j.jhazmat.2019.121917.

[41] Kumar, M., Ansari, M.N.M., Boukhris, I., Al-Buriahi, M.S., Alrowaili, Z.A., Alfryyan, N., Thomas, P., and Vaish, R., (2022). Sonophotocatalytic Dye Degradation Using rGO-$BiVO_4$ Composites, Glob. Chall. 6, 2100132. https://doi.org/10.1002/gch2.202100132.

[42] Tahir, M.B., Iqbal, T., Kiran, H., and Hasan, A., (2019). Insighting role of reduced graphene oxide in $BiVO_4$ nanoparticles for improved photocatalytic hydrogen evolution and dyes degradation, Int J Energy Res 43, 2410–2417. https://doi.org/10.1002/er.4443.

[43] Liu, S. Pan, J., Kong, W., Li, X., Zhang, J., Zhang, X., Liu, R., Li, Y., Zhao, Y., Wang, D., Zhang, J., and Zhu, S., (2022). Synergetic nanoarchitectonics of defects and cocatalysts in oxygen- vacancy-rich $BiVO_4$/reduced graphene oxide mott-schottky heterostructures for photocatalytic water oxidation, ACS Appl Mater Interfaces 14, 12180–12192. https://doi.org/10.1021/acsami.1c22250.

[44] Yaw, C.S., Ng, W.C., Ruan, Q., Tang, J., Soh, A.K., and Chong, M.N., (2020). Tuning of reduced graphene oxide thin film as an efficient electron conductive interlayer in a proven heterojunction photoanode for solar-driven photoelectrochemical water splitting, J Alloys Compd 817, 152721. https://doi.org/10.1016/j.jallcom.2019.152721.

[45] Shao, S., Zhang, J., Li, L., Qin, Y., Liu, Z.Q., and Wang, T., (2022). Visible-light-driven photocatalytic N_2 fixation to nitrates by 2D/2D ultrathin $BiVO_4$ nanosheet/rGO nanocomposites, Chem. Commun. 58, 2184–2187. https://doi.org/10.1039/d1cc06750h.

[46] Cai, J., Zhao, Q., Hsu, W.-Y., Choi, C., Liu, Y., Martirez, J.M.P., Chen, C., Huang, J., Carter, E.A., and Huang, Y., (2023). Highly selective electrochemical reduction of CO_2 into methane on nanotwinned Cu, J Am Chem Soc 145, 9136–9143. https://doi.org/10.1021/jacs.3c00847.

DOI: 10.62184/acj.jacj1000202420

[47] Matsubara, Y., (2017). Standard electrode potentials for the reduction of CO_2 to CO in acetonitrile–water mixtures determined using a generalized method for proton-coupled electron-transfer reactions, ACS Energy Lett 2, 1886–1891. https://doi.org/10.1021/acsenergylett.7b00548.

[48] Chen, L., Zhang, M., Yang, J., Li, Y., Sivalingam, Y., Shi, Q., Xie, M., and Han, W., (2019). Synthesis of $BiVO_4$ quantum dots/reduced graphene oxide composites for CO_2 reduction, Mater Sci Semicond Process 102, 104578. https://doi.org/10.1016/j.mssp.2019.06.013.

[49] Ghani, N., Iqbal, J., Sadaf, S., Nawaz Bhatti, H., and Asgher, M., (2020). Comparison of photo-esterification capability of bismuth vanadate with reduced graphene oxide bismuth vanadate (RGO/$BiVO_4$) composite for biodiesel production from high free fatty acid containing non-edible oil, Chemistry Select 5, 9245–9253. https://doi.org/10.1002/slct.202001913.